# Experimental ocean acidification alters the allocation of metabolic energy

T.-C. Francis Pan[1], Scott L. Applebaum[1], and Donal T. Manahan[2]

Department of Biological Sciences, University of Southern California, Los Angeles, CA 90089

Edited by George N. Somero, Stanford University, Pacific Grove, CA, and approved March 4, 2015 (received for review September 2, 2014)

**Energy is required to maintain physiological homeostasis in response to environmental change. Although responses to environmental stressors frequently are assumed to involve high metabolic costs, the biochemical bases of actual energy demands are rarely quantified. We studied the impact of a near-future scenario of ocean acidification [800 μatm partial pressure of $CO_2$ ($pCO_2$)] during the development and growth of an important model organism in developmental and environmental biology, the sea urchin *Strongylocentrotus purpuratus*. Size, metabolic rate, biochemical content, and gene expression were not different in larvae growing under control and seawater acidification treatments. Measurements limited to those levels of biological analysis did not reveal the biochemical mechanisms of response to ocean acidification that occurred at the cellular level. In vivo rates of protein synthesis and ion transport increased ∼50% under acidification. Importantly, the in vivo physiological increases in ion transport were not predicted from total enzyme activity or gene expression. Under acidification, the increased rates of protein synthesis and ion transport that were sustained in growing larvae collectively accounted for the majority of available ATP (84%). In contrast, embryos and prefeeding and unfed larvae in control treatments allocated on average only 40% of ATP to these same two processes. Understanding the biochemical strategies for accommodating increases in metabolic energy demand and their biological limitations can serve as a quantitative basis for assessing sublethal effects of global change. Variation in the ability to allocate ATP differentially among essential functions may be a key basis of resilience to ocean acidification and other compounding environmental stressors.**

ocean acidification | sea urchin | energetics | metabolic allocation | development

Studies of biological responses to future scenarios of global change are of significant interest, given the most recent projections of future environmental conditions (1). In addition to important impacts in the atmosphere and on terrestrial systems, anthropogenic $CO_2$ emission is causing acidification of the world's oceans (2, 3). Determining the biological responses to ocean acidification is a critical component of the study of how marine ecosystems may be altered under future scenarios of anthropogenic global environmental change. Predicting the potential for evolutionary adaptation to global change requires an understanding of the biochemical mechanisms that maintain homeostasis of physiological systems (4, 5).

The developmental stages of many marine organisms have evolved cellular defenses to mitigate the impact of current environmental stressors (6). Whether these protective mechanisms can respond to future, rapid anthropogenic changes is still an open question. Marine invertebrate larvae, and particularly those with calcareous structures, have been used in numerous investigations of the biological impact of ocean acidification (2, 7–10). Although the magnitude of a response appears to be species specific, acidification can, to varying degrees, impact a wide range of biological processes in developmental forms (7–14). For instance, under near-future global mean $CO_2$ conditions [720–1,000 μatm partial pressure of $CO_2$ ($pCO_2$)] (1), species of larval sea urchins generally are reduced in size by 10% or less (7, 9, 15–17), but studies of metabolic rate and ion regulation suggest that acidification may result in increased metabolic costs to maintain homeostasis (11, 12). By studying responses to seawater acidification at several levels of biological organization during the development of the sea urchin, *Strongylocentrotus purpuratus*—from whole-organism growth, to macromolecular synthesis rates, enzyme activities, and gene expressions—we show that, although the impact of acidification at the organismal level is minimal, dramatic compensation occurs at the cellular level. Specifically, growth is maintained by changes in energy allocation to accommodate the costs required to sustain increases in protein synthesis and ion transport. We conclude that measurements limited to morphological characteristics, metabolic rate, biochemical content, and gene expression do not reveal the major biochemical response mechanisms underlying the apparent resilience to acidification in developing sea urchins.

## Results

**Size and Metabolic Rate.** Body length (Fig. 1*A*) was measured during 14 d of development and growth in control and acidified seawater (Table S1). Midline body length (mean ± SEM) increased from 109.7 ± 0.6 μm on day 1 to 363.8 ± 3.1 μm on day 14 and did not differ between control and acidification treatments of larvae fed ad libitum (ANCOVA, $P = 0.095$, $n = 2{,}081$) (Fig. 1*A*) and unfed larvae (ANOVA, $P = 0.537$, $n = 481$). Metabolic rates (measured as oxygen consumption; see *Discussion* for oxyenthalpic equivalents) did not differ significantly between control and acidification treatments in fed larvae (ANCOVA,

### Significance

**Anthropogenic emission of $CO_2$ is causing global ocean acidification. For many species, biological responses to acidification often show limited impact at the level of the whole animal. Our integrative studies of whole-organism growth and metabolic rates, rates of protein synthesis and ion transport, enzyme activity, and gene expression show that although the organismal-level impact of acidification on developing sea urchins was minimal, dramatic compensation occurred at the cellular level. Increased rates of synthesis and ion transport resulted in 84% of available energy being allocated to those processes under acidification. Defining the limits of differential energy allocation for the maintenance of critical physiological functions in response to compounding stressors will help provide a mechanistic understanding of resilience potential to environmental change.**

Author contributions: T.-C.F.P., S.L.A., and D.T.M. designed research; T.-C.F.P. and S.L.A. performed research; T.-C.F.P., S.L.A., and D.T.M. contributed new reagents/analytic tools; T.-C.F.P., S.L.A., and D.T.M. analyzed data; and T.-C.F.P., S.L.A., and D.T.M. wrote the paper.

The authors declare no conflict of interest.

This article is a PNAS Direct Submission.

Freely available online through the PNAS open access option.

[1]T.-C.F.P. and S.L.A. contributed equally to this work.

[2]To whom correspondence should be addressed. Email: manahan@usc.edu.

This article contains supporting information online at www.pnas.org/lookup/suppl/doi:10.1073/pnas.1416967112/-/DCSupplemental.

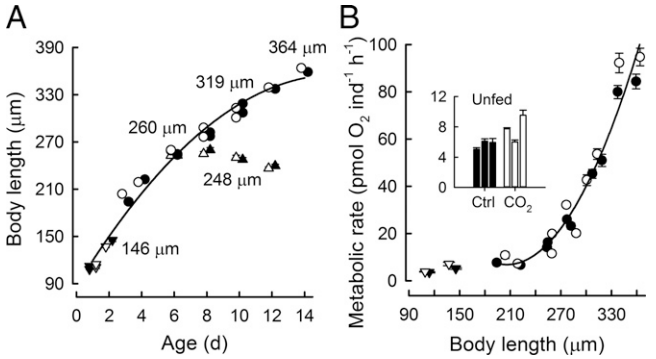


**Fig. 1.** Size (*A*) and metabolic rate (*B*) in developing sea urchins under control (closed symbols) and seawater acidification (open symbols) treatments. (*A*) Changes in diameters of embryos (inverted triangles), body lengths of larvae (circles) and unfed larvae (triangles). Each data point represents mean ± SEM ($n = 50$ individuals). Where not visible, error bars fall within the graphical representation of the data point. For visual clarity, data points for a given *x*-axis value are slightly offset when symbols overlap. Body lengths did not differ between control and acidification treatments for fed (ANCOVA, $P = 0.095$, $n = 2{,}081$) and unfed ($P = 0.537$, $n = 481$) larvae. (*B*) Metabolic rate (measured as $O_2$ consumption) per individual as a function of body length. Error bars represent 1 SEM, $n = 8$–10 respiration assays. (*Inset*) Bar graph shows replicate measurements on 6-, 8-, and 10-d-old unfed larvae under control (Ctrl) and acidification ($CO_2$) treatments. Metabolic rates did not differ significantly between control and acidification treatments for fed larvae (ANCOVA, $P = 0.326$, $n = 255$). Metabolic rates of embryos and unfed larvae were elevated under acidification (ANOVA, $P < 0.001$, $n = 97$).

$P = 0.326$, $n = 255$) (Fig. 1*B*). Metabolic rates of embryos (Fig. 1*B*) and 6- to 10-d-old unfed larvae (Fig. 1*B*, *Inset*) were elevated under acidification (ANOVA, $P < 0.001$, $n = 97$). This increase in metabolic rates was 24% on average for embryos and 37% on average for unfed larvae.

**Protein Content, Synthesis, and Turnover Rates.** Acidification did not affect whole-body protein content of any developmental stage studied (embryos and unfed larvae, ANOVA, $P = 0.063$, $n = 49$; feeding larvae, ANCOVA, $P = 0.847$, $n = 49$) (Fig. 2*A*). The mole-percent amino acid composition of protein did not differ between control and acidification treatments (Table S2). In contrast, increases in absolute rates of protein synthesis were evident under acidification treatment from the earliest larval stage studied (194 μm, 3-d-old) (Fig. 2*B*). A regression of protein synthesis rate on size shows that growing sea urchin larvae under acidification had an average increase of 1.6-fold in size-specific rates of protein synthesis during the larval period tested (ANCOVA, $P = 0.009$, $n = 20$) (Fig. 2*B*). From a post hoc analysis of developmental stages with no growth (embryos and unfed larvae), seawater acidification resulted in a 2.0-fold increase in protein synthesis rates in 6- to 10-d-old unfed larvae ($P < 0.001$, $n = 12$; ANOVA in Table S3) (Fig. 2*B*, *Inset*) and showed no difference for 1- and 2-d-old embryos ($P = 0.953$, $n = 8$). These increases in rates of protein synthesis (Fig. 2*B*) represent turnover, because protein content did not change (Fig. 2*A*). Electrophoretic analyses of larval proteins showed that, even though the rate of protein synthesis increased under acidification (Fig. S1*A*), the size distribution and pattern of synthesized proteins (shown by $^{35}$S-Met/Cys labeling) appear unchanged in 12-d-old, fed larvae (Fig. S1*B*). The analyses presented here support the conclusion that the increased rates of protein turnover involved all molecular weight classes of proteins observable at the resolution of 1D gel electrophoresis. The impact of seawater acidification on the processes of protein metabolism is illustrated in Fig. S2. Calculation of protein depositional efficiency (the ratio of protein accreted to protein synthesized) revealed that acidification resulted in a lower efficiency of protein deposition (21.2%) relative to controls (34.3%) for larvae of a given size. Combined, these analyses (Fig. 2 and Figs. S1 and S2) show that the balance between increased rates of protein synthesis and decreased protein depositional efficiency is an important mechanism for maintaining protein growth under simulated ocean acidification.

**Metabolic Cost of Protein Synthesis.** The cost of protein synthesis was determined for embryos and larvae of *S. purpuratus* reared under control and acidification treatments. The energy cost per unit protein synthesized is determined from concurrent measurements of changes in protein synthesis and metabolic rates in the presence and absence of emetine, a specific inhibitor of protein synthesis (18). Oxygen consumption was converted to energy using an oxyenthalpic equivalent of 484 kJ/mol $O_2$, an average value based on lipids and proteins (19) that are the major biochemical constituents of developmental stages of *S. purpuratus* (20). From the simultaneous reduction in protein synthesis and metabolic rates, the cost of protein synthesis was calculated in 1-d-old blastulae (Fig. 3 *A* and *B*). This analysis was extended to a series of developmental stages, and the cost of protein synthesis in developing sea urchins was calculated to be 2.4 ± 0.21 J/mg protein synthesized (grand mean, $n = 9$) (Fig. 3*C*). Important for calculations of energy allocation to protein synthesis under control and acidification treatments is that the cost of synthesizing a unit-mass of protein did not differ between treatments ($P = 0.304$, *t* test, $n = 3$ for each treatment) (Fig. 3*C*; see *SI Materials and Methods* for details of biological and technical replications).

**Ion Transport Rate, Enzyme Activity, and Gene Expression of $Na^+$,$K^+$-ATPase.** Measurements of $Na^+$,$K^+$-ATPase were made at three levels: in vivo physiological activity, total biochemical activity, and gene expression. The physiologically active fraction of total $Na^+$,$K^+$-ATPase (herein referred to as "ion transport," i.e., in vivo $Na^+$,$K^+$-ATPase activity) was measured as the difference in transport rate of rubidium ($^{86}Rb^+$, a physiological analog of $K^+$) in the

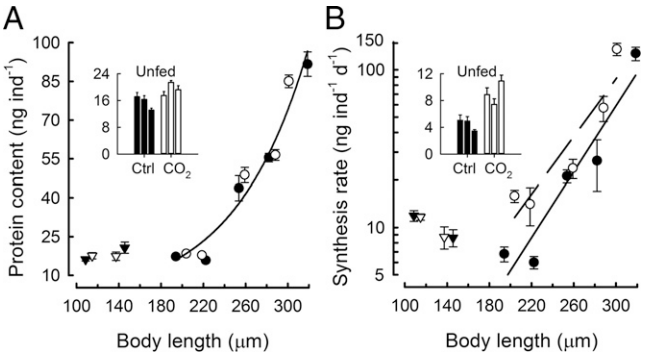


**Fig. 2.** Protein content and synthesis in developing sea urchins under control (closed symbols) and seawater acidification (open symbols) treatments. (*A*) Protein content as a function of body length in embryos (triangles) and fed larvae (circles). Error bars indicate 1 SEM, $n = 4$–5 protein assays. Where not visible, error bars fall within the graphical representation of the data point. No statistical differences in protein content were observed between control and acidification treatments (embryos and unfed larvae, ANOVA, $P = 0.063$, $n = 49$; feeding larvae, ANCOVA, $P = 0.847$, $n = 49$). (*Inset*) The bar graph shows replicate measurements on 6-, 8-, and 10-d-old unfed larvae. (*B*) Each data point represents a protein synthesis rate, calculated from the combined slope (± SE) of duplicate six-point time-course assays of the amount of protein synthesized, corrected for intracellular specific activity of $^{14}$C-alanine in the free amino acid pool. Size-specific protein synthesis rates were significantly greater under acidification in growing larvae (ANCOVA, $P = 0.009$, $n = 20$) and (*Inset*) in unfed larvae (Post hoc test, $P < 0.001$, $n = 12$). See Fig. S2 for equations for the regression lines shown here in *A* and *B*.

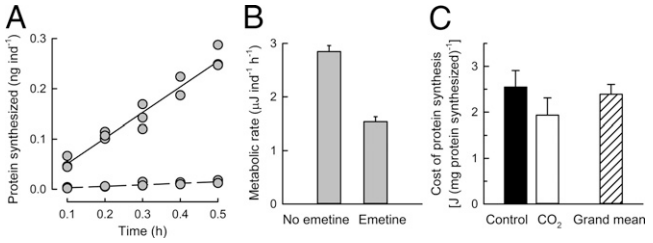


**Fig. 3.** Energy cost of protein synthesis in developing sea urchins. (*A*) Protein synthesis of 1-d-old embryos in the absence (solid regression line, rate = 0.51 ± 0.032 nanograms per individual per hour, slope ± SE of slope) and presence (dashed regression line, rate = 0.03 ± 0.004 nanograms per individual per hour) of 100 μM emetine. Synthesis rates were calculated from triplicate, five-point time-course assays. (*B*) Metabolic rate measured as oxygen consumption, for the cohort of embryos in *A*, converted to energy equivalents (expressed in microJoules). Error bars represent 1 SEM, $n = 8$ respiration assays. (*C*) The cost of protein synthesis was calculated from the simultaneous decreases in protein synthesis and metabolic rate under inhibition by emetine. Error bars represent 1 SEM. The energy cost of protein synthesis did not differ significantly between control (black bar, $n = 3$) and seawater acidification (open bar, $n = 3$) treatments (*t* test, $df = 4$, $t = 1.178$, $P = 0.304$). The grand mean (hatched bar) of 2.4 ± 0.21 J/mg protein synthesized was calculated from all cost determinations ($n = 9$) for two $pCO_2$ treatments and developmental stages spanning 1-d-old embryos to 10-d-old larvae.

presence and absence of ouabain (Fig. 4*A*). A regression of ion transport rates on size shows that growing sea urchin larvae under acidification had an 1.4-fold increase in the size-specific ion transport rate (ANCOVA, $P = 0.016$, $n = 20$) (Fig. 4*B*). A post hoc analysis of developmental stages with no growth (embryos and unfed larvae) showed that the ion transport rates increased 2.3-fold in unfed larvae under acidification ($P = 0.001$, $n = 8$; ANOVA in Table S3) (Fig. 4*B*, *Inset*) and showed no difference in 1- and 2-d-old embryos ($P = 0.852$, $n = 8$). In contrast to the significant increases in physiological rates of ion transport under acidification, no concurrent changes in total enzyme activity (ANOVA, $P = 0.877$, $n = 38$) (Fig. 4*C*) were observed in pre-feeding or fed larvae. Additionally, *$Na^+$,$K^+$-ATPase* gene expression did not reflect the direction of measured changes in rates of ion transport. There is a marginally significant effect of acidification on *$Na^+$,$K^+$-ATPase* gene expression (ANOVA, $P = 0.049$, $n = 48$) (Fig. 4*C*). Post hoc analysis showed that this effect was driven only by changes in 4-d-old larvae ($P < 0.001$, $n = 3$). All other ages showed no differences in gene expression under acidification relative to controls. Although differences were seen in 4-d-old larvae, the ranking was reversed: Gene expression was lower under acidification relative to controls, in contrast to the increased physiological rate of ion transport. Under our experimental conditions, regulation of $Na^+$,$K^+$-ATPase takes place primarily at the physiological level rather than at the biochemical or molecular biological levels.

**Changes in Energy Allocation in Response to Seawater Acidification.** Protein synthesis and $Na^+$,$K^+$-ATPase together accounted for the majority of the allocation of metabolic energy throughout the period of growth and development studied (Fig. 5). The data and calculations that form the basis of Fig. 5 are given in Table S4 and in *SI Calculations and Estimations*. The proportion of ATP used for these two major energy-requiring processes increased with the transition to exogenous feeding and the commencement of growth, as well as with acidification treatment for all stages tested (with the exception of the earliest developmental stages tested, 2-d-old embryos). For embryos and prefeeding and unfed larvae—stages at which no growth occurred—an average of 40% of total ATP was devoted to protein synthesis and ion transport under control conditions (Fig. 5 *A* and *B*). In contrast, the allocation of total ATP for protein synthesis and ion transport increased to 55% in fed growing larvae. Importantly, acidification increased the average ATP allocation to protein synthesis and ion transport from 40 to 62% for prefeeding stages and unfed larvae and from 55 to 84% for feeding larvae (Fig. 5). A noteworthy pattern is evident in which the unaccounted fraction of total ATP decreased gradually from 53% in 2-d-old larvae to 14% in10-d-old larvae under continuous exposure to seawater acidification (Fig. 5*A*). This decrease in the unaccounted fraction of total ATP can be considered energy that is no longer available to support the demands of routine maintenance metabolism or the ability to respond to other stressors. Again, we emphasize that the major changes in ATP allocation in response to seawater acidification are not reflected by midline body lengths (Fig. 1*A*), gross morphological characteristics (Fig. 5*C*), metabolic rate (Fig. 1*B*), protein content (Fig. 2*B*), enzyme activity (Fig. 4*C*), or gene expression (Fig. 4*C*).

## Discussion

The developmental stages of sea urchins have been used routinely to study biological responses to ocean acidification and to other environmental stressors (6, 9, 10). Often, additional metabolic costs are invoked as an explanation for physiological responses to ocean acidification (11, 12, 21). In the present study we show that, for sea urchins growing at the lower range (~800 μatm) of the near-future $pCO_2$ level projected by the Intergovernmental Panel on Climate Change (IPCC) (RCP6.0 in ref. 1; further details are given in Table S1), no changes were observed in growth rate, metabolic rate, biochemical composition, or the amount of $Na^+$,$K^+$-ATPase. The response to acidification was dramatic but occurred at other levels of biological

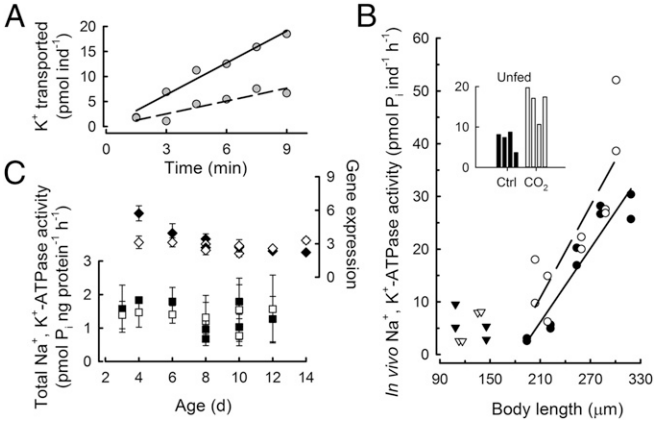


**Fig. 4.** Ion transport rate, total enzyme activity, and gene expression of $Na^+$,$K^+$-ATPase in developing sea urchins. (*A*) In vivo $Na^+$,$K^+$-ATPase activity was determined from $^{86}Rb^+$ transport rates, corrected for the specific activity of $K^+$ in seawater, in the absence (solid regression line, rate = 2.1 ± 0.19 picomoles $K^+$ per individual per minute, slope ± SE of slope) and presence (dashed regression line, rate = 0.9 ± 0.18 picomoles $K^+$ per individual per minute) of 2 mM ouabain. (*B*) In vivo $Na^+$,$K^+$-ATPase activity under control (closed symbols) and seawater acidification (open symbols) treatments in embryos (triangles) and larvae (circles) as a function of body size. Each data point was calculated from time-course assays as shown in *A*. (*Inset*) The bar graph shows duplicate measurements on 6- and 8-d-old unfed larvae. Seawater acidification treatment significantly increased in vivo $Na^+$,$K^+$-ATPase activity in growing larvae (ANCOVA, $P = 0.016$, $n = 20$) as well as in unfed larvae (*Inset*). Post hoc test, $P = 0.001$, $n = 8$. (*C*) Relative $Na^+$,$K^+$-ATPase gene expression and total enzyme activity. Error bars indicate 1 SEM, $n = 3$–4 assays. Where not visible, error bars fall within the graphical representation of the data point. No statistical differences in gene expression or total enzyme activity occurred between control and acidification treatments, with the exception of 4-d-old larvae (~220 μm). For this stage, gene expression did not predict the changes in physiological rates of ion transport (*B*), because gene expression was higher in the control relative to acidification treatment (post hoc test, $P < 0.001$).

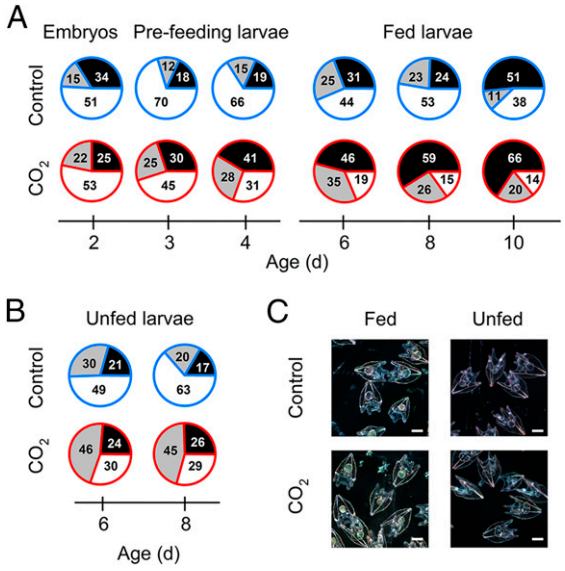


**Fig. 5.** Changes in ATP allocation to protein synthesis (black), in vivo $Na^+,K^+$-ATPase activity (gray), and the unaccounted fraction of total ATP (white) in developing sea urchins. (*A* and *B*) Metabolic energy budgets for embryos, prefeeding, and fed larvae (*A*) and unfed larvae (*B*) under control (outlined in blue) and seawater acidification and $CO_2$ (outlined in red) treatments. Values within each pie chart indicate the proportion (%) of the total metabolic rate allocated to each category. Data used for calculation of ATP allocation are given in Table S4. (*C*) Images of 6-d-old fed and unfed larvae under control and acidification treatments. (Scale bars: 100 μm.)

analysis. Our results for larval size are in general agreement with another study showing that *S. purpuratus* exposed to 900 μatm $pCO_2$ had an ∼5% reduction in body length but reporting notable changes in allele frequency and gene expression (17). In our study, we also noted no changes in body length but did observe an acidification-induced increase of ∼50% in the rates of protein synthesis and ion transport. Protein growth was maintained by changing the balance between increased rates of protein synthesis and decreased protein depositional efficiency. Our findings support prior work showing that ocean acidification does not affect protein content (22) but highlight the critical need to study the mechanisms and dynamics of biosynthesis, which undergo dramatic changes to compensate for the maintenance of biochemical content during growth. Similarly, our results show that increases in ion transport by $Na^+,K^+$-ATPase and the concomitant increase in ATP demand were not predicted by changes in the expression of the gene coding for that protein or by changes in the amount of total enzyme.

A major conclusion from our work is that the primary metabolic mechanism to respond to ocean acidification in growing sea urchin larvae is a change in allocation within a fixed amount of total ATP to support increased protein synthesis and ion transport. Combined, protein synthesis and ion transport accounted for an average of 84% of the metabolic rate of feeding larvae under acidification, compared with 55% in controls. This ∼30% difference in the allocation of metabolic energy could reduce an organism's ability to respond to additional energy-demanding environmental stressors and has more general implications for the ability to sustain fundamental biochemical processes (23). For instance, even a relatively small energy requirement for responses to environmental toxicants (24) and other macromolecular synthesis requirements [e.g., RNA (25)] could be constrained by changes in ATP allocation. A comprehensive accounting of the variations in each of the major processes supported by total ATP would improve predictions from models attempting to understand biological responses to ocean acidification and other compounding environmental stressors.

**Biochemical Rate Compensation Under Acidification.**

***Protein synthesis.*** Ocean acidification increased the rates of protein synthesis, described in this study as the linear regressions of size-specific synthesis rates with parallel slopes but with different intercepts (Fig. 2*B*). Because there were no differences in protein growth between treatments (Fig. 2*A*), this ∼50% elevation in protein synthesis throughout the developmental and growth period studied represents an increase in protein turnover. This increase in protein turnover was analyzed further by calculating protein depositional efficiency (Fig. S2). The size-specific protein depositional efficiency of 34% in larvae of *S. purpuratus* (270 μm) (Fig. S2) under control conditions agrees well with previously published values for another species of sea urchin, *Lytechinus pictus*, which range from 21% to 37% depending on developmental stage (18). Additionally, the value we report of ∼2%/h for fractional rates of protein turnover in embryonic stages of *S. purpuratus* (*SI Calculations and Estimations*) is consistent with earlier measurements (26), confirming the validity of our techniques and measurements. This increase in protein synthesis under acidification was not limited to a specific size-class of proteins (Fig. S1*B*). What might be the basis for an up-regulation of synthesis and turnover for so many different proteins? Future research to elucidate the cellular mechanisms of acidification-induced increases in protein synthesis and turnover could focus on the degradation of newly synthesized proteins (27), polypeptide elongation rates (and possible early truncation) on isolated ribosomes (28), or the precision of translation and folding of polypeptides (29). Each of these processes requires considerable amounts of ATP (30). Whatever the specific mechanism, the regulation of protein synthesis and turnover clearly are primary drivers of the changes in ATP allocation under ocean acidification.

Compensating for decreased depositional efficiency (Fig. S2) and increased protein turnover necessitated higher rates of protein synthesis (Fig. 2*B*), with significant consequences for use of ATP. The essential first step in being able to quantify these impacts was to measure the cost of protein synthesis for early developmental stages of *S. purpuratus* (Fig. 3). The value we report of 2.4 J/mg protein synthesized is within the range of published values for protein synthesis costs in animals (18, 31–36). The integrative analysis of biochemical and physiological processes we present in this study permits the calculation of stage-specific ATP allocation to protein synthesis during sea urchin development (Fig. 5). Importantly, the cost of protein synthesis in *S. purpuratus* has a fixed value that is independent of the developmental stages studied and the levels of $pCO_2$ tested (Fig. 3*C*). Developmental stages responded to ocean acidification by increasing protein synthesis rates and hence the allocation of ATP to protein synthesis but not by altering the cost of synthesizing a unit-mass of protein.

***Ion regulation.*** A second mechanism contributing to increased ATP demand under acidification is the regulation of ion transport (Figs. 4 and 5). For all the developmental stages and feeding treatments investigated, ion transport accounted for between 11% and 30% of the metabolic rate, a range that increased to 20–46% under acidification (Fig. 5). The increase of in vivo $Na^+,K^+$-ATPase activity may be related to acid–base regulation (37). For marine invertebrates, acid–base regulation is an important response mechanism to ocean acidification (12, 38). Additionally, higher in vivo $Na^+,K^+$-ATPase activity may be related to enhanced sodium-dependent amino acid transport (39) to support increased protein synthesis under acidification.

Importantly, these significant changes in the demand for ATP to support increased rates of ion transport were not detectable by either total enzyme assays or changes in gene expression (Fig. 4*C*). There is growing evidence that transcript levels often are

uncoupled from the amounts of proteins they encode. For example, recent large-scale transcriptomic and proteomic studies of the expression of ~5,000 genes and their corresponding proteins have shown that changes in gene expression are not good measures of protein abundance (40). Even when mRNA predicts protein abundance, physiologically relevant protein activity can vary substantially from patterns of gene expression or protein abundance (41–44). For comparative studies of marine organisms that lack comprehensive and simultaneous quantification of transcriptomes and proteomes (40), analyses that infer physiological activity from measurements of gene expression should be interpreted with caution.

***Allocation of metabolic energy***. We base our calculations of total metabolic expenditure on measurements of oxygen consumption. There is an extensive literature on the calculations of energetic and biochemical equivalents of respiratory oxygen consumption (thermodynamic and oxyenthalpic energy equivalents) (19). Measurements conducted using direct calorimetry (heat-dissipation rates) and indirect calorimetry (rates of oxygen consumption) on 31 species, including early stages of marine animals, have shown that under normoxic conditions the oxyenthalpic equivalent is fully aerobic, at 463 ± 39 kJ/mol $O_2$ (45). Hence, under normoxic condition, a measured rate of oxygen consumption accounts for all interconvertible energy equivalents, independent of the specific biochemical pathways involved. Metabolic energy budgets in the current study were calculated based on the oxyenthalpic equivalent of 484 kJ/mol $O_2$, an average value for lipid and protein (19, 20). Here, we use ATP as the energy equivalent for the calculation of metabolic allocation (Fig. 5 *A* and *B*).

A dramatic finding from this analysis of metabolic allocation is that 84% of the available ATP pool is accounted for by the cost of protein synthesis and ion regulation under acidification conditions (Fig. 5). This surprising capacity to respond to sublethal environmental stresses for an extended period (tested for 10 d) eclipses the fact that the ATP allocation in control conditions is consistent with existing literature. For instance, the summary diagram of ATP-demanding processes given in Hochachka and Somero (ref. 23, p. 28) shows that ~30% of ATP is allocated to protein synthesis and ~30% to regulate sodium–potassium flux. These values are similar to those we report for developmental stages in this article: On average, we found that protein synthesis accounted for 27% of ATP, and sodium–potassium pump activity accounted for 19% (Fig. 5). Notably, our measurements reported here are consistent with the range of previously reported values for these processes during sea urchin development (18, 46). The sustainability of the high allocation of ATP under environmental stress, the long-term impact on organismal performance, and the ability to support other essential physiological processes are important themes for future research.

**Feeding State Alters Metabolic Rates Under Acidification.**

***Metabolic responses of unfed larvae***. When larvae developed to the feeding stage (4 d old) but subsequently were unfed through day 10, metabolic rates did increase in response to acidification (Fig. 1*B*, *Inset*). It is noteworthy that an increase in metabolic rate—an increase driven entirely by protein synthesis and ion transport—occurred under acidification only for larvae under conditions of food limitation (*SI Calculations and Estimations*). In the absence of growth in unfed larvae, such metabolic responses likely represent the costs of maintenance under acidification. The mechanisms underlying the differential energy response to the stress of ocean acidification between fed and unfed larvae require further study but likely are related to different anabolic (growth) and catabolic (starvation) states. The difference in metabolic response between fed and unfed larvae suggests that nutritional and physiological states impact the response to many environmental stressors, including ocean acidification (47). Such increases in metabolic demand have important implications for long-term resistance to starvation of larval forms with minimal energy reserves (48, 49).

***Metabolic responses of fed larvae***. Once larvae reach feeding competence and are provided with food, rapid growth ensues (Fig. 1*A*). The metabolic cost of such growth is high in the developmental stages. For instance, in another species of sea urchin, *L. pictus*, up to 75% of the available ATP pool is allocated to protein synthesis during growth (18). Clearly the large energy requirements for growth, even under ad libitum feeding conditions, greatly constrain the capacity to change ATP allocation under environmental stress. The continuous increase in metabolic rate per individual during growth may allow an accommodation to increased energy demand of major energy-consuming biochemical processes under acidification. A lack of difference in the metabolic rates of larvae under control and acidification treatments belies the substantial differences in ATP allocation. Such cellular changes were not revealed by measurements of oxygen consumption on whole organisms, because changes in ATP allocation were accommodated without an increase in metabolic rate (Fig. 1*B*). These findings demonstrate that a lack of increase in metabolic rate in response to acidification should not be interpreted to mean that an environmental perturbation has no impact on an organism.

Remarkably, it appears that sea urchin larvae can allocate on average 84% of their total ATP to just two processes without any immediate, negative impact on growth. The physiological limits in the ability of larvae to respond to ocean acidification without increasing metabolic rates may occur at higher $pCO_2$. Such a suggestion is consistent with the findings of an increase in metabolic rates in feeding larvae of *S. purpuratus* in the presence of $pCO_2$ levels higher than the 800 μatm tested in the current study (11, 16). Future studies of biological responses that focus on differential allocation of ATP could help identify and predict the limits of physiological resilience to compounding interactions of ocean acidification, temperature, food availability, and other consequences of global change.

***Tradeoffs of ATP allocation—a basis for physiological resilience***. Ocean acidification experiments often show limited impact at the level of the whole organism. Our results demonstrate that major compensatory responses occur at the cellular level, even when whole-organism responses are minimal. A long-standing question in metabolic regulation is at what point sublethal stress becomes lethal because of energy limitation (21, 23). Our findings of changes in ATP allocation within a tightly constrained energy budget have important implications for organismal resilience. Under changing environments, in which ATP demand may exceed metabolic capacity, individuals with maintenance costs less sensitive to environmental stressors are more likely to survive. Genetically determined variations in the ability to allocate ATP likely will influence the resilience of individuals and the adaptive potential of populations in a changing environment (5). Physiologically, it is important to define the hierarchy of ATP-consuming processes that support the maintenance of essential functions under benign and stressful conditions. The ability to measure the associated metabolic costs, tradeoffs, and limits to ATP allocation to support critical cellular functions will help provide a mechanistic understanding of resilience potential to global change.

## Materials and Methods

**General Approach and Rationale.** We used an integrative biological approach to study the biochemical and physiological responses to seawater acidification in developing sea urchins. Details of each specific method are given in *SI Materials and Methods*. In brief, in vivo measurements of metabolic rates, protein synthesis rates, and ion transport rates of $Na^+$,$K^+$-ATPase were conducted. These were complemented with measurements of larval size, in vitro analyses of protein content, total $Na^+$,$K^+$-ATPase enzyme activity, and $Na^+$,$K^+$-ATPase gene expression. To enable the calculation of absolute rates of protein synthesis, individuals at selected ages from control and acidification treatments were analyzed for the mole-percent amino acid composition and for the

calculation of the average molecular mass of whole-body total protein (Table S2). A series of experiments was undertaken to determine the energy cost of protein synthesis. The integration of this suite of measurements was used to determine the major biochemical processes responsible for differential energy allocation in response to ocean acidification.

**Sea Urchin Culturing and $CO_2$ Treatments.** Adult sea urchins (*S. purpuratus*) were induced to spawn by intracoelomic injection of 0.5 M KCl. Gametes from males and females were pooled and allowed to fertilize in filtered (pore size, 0.2 μm) seawater at 15 °C (*SI Materials and Methods*). Eggs from individual females were pretested for fertilization and were used for experiments only if more than 95% fertilization success was observed. For each treatment, newly fertilized eggs were placed in 200-L cylindrical culture vessels equipped with motorized stirring paddles providing slow vertical movement. Cultures were stocked at an initial density of 20 eggs/mL. Control-group cultures were aerated continuously with ambient, atmospheric air. Seawater acidification treatments were aerated with a premixed, compressed air source supplemented with $CO_2$ (Gilmore Air) to yield an average $pCO_2$ of 800.6 ± 9.07 μatm based on daily measurements from each culture vessel (Table S1). The $pCO_2$ levels used reflect present-day and near-future IPCC projections (~800 μatm) (1). A complete water change was performed for all culture vessels every 2 d. Water was replaced with fresh seawater that had been pre-equilibrated to the appropriate temperature and $CO_2$ treatment level. At the onset of exogenous feeding, 4-d-old larvae from both the control and acidification treatments were stocked in 20-L culture vessels at a starting concentration of 10 larvae/mL into fed and unfed treatments; larvae numbers decreased to ~2/mL because of sampling during the course of experiments. Larvae were kept in suspension with rotary motorized stirrers. Fed treatments (ad libitum) were supplied with the algae *Rhodomonas lens* at 30,000 cells/mL, and food was replenished daily. Seawater acidification experiments were replicated with gametes obtained from different sets of adults (i.e., different larval cohorts; see *SI Materials and Methods*).

**ACKNOWLEDGMENTS.** We thank Drs. D. Hedgecock and C. Frieder for helpful comments on the manuscript and C. Capron, R. Sawyer, T. Hild, and B. Lentz for technical assistance. This work was supported by National Science Foundation Grant Emerging Frontiers 1220587.

1. Clarke L, et al. (2014) *Climate Change 2014: Mitigation of Climate Change. Contribution of Working Group III to the Fifth Assessment Report of the Intergovernmental Panel on Climate Change*, eds Edenhofer O, et al. (Cambridge Univ Press, Cambridge, New York).
2. Feely RA, et al. (2004) Impact of anthropogenic $CO_2$ on the $CaCO_3$ system in the oceans. *Science* 305(5682):362–366.
3. Hönisch B, et al. (2012) The geological record of ocean acidification. *Science* 335(6072): 1058–1063.
4. Somero GN (2010) The physiology of climate change: How potentials for acclimatization and genetic adaptation will determine 'winners' and 'losers'. *J Exp Biol* 213(6): 912–920.
5. Applebaum SL, Pan TCF, Hedgecock D, Manahan DT (2014) Separating the nature and nurture of the allocation of energy in response to global change. *Integr Comp Biol* 54(2):284–295.
6. Hamdoun A, Epel D (2007) Embryo stability and vulnerability in an always changing world. *Proc Natl Acad Sci USA* 104(6):1745–1750.
7. Byrne M (2011) Impact of ocean warming and ocean acidification on marine invertebrate life history stages: Vulnerabilities and potential for persistence in a changing ocean. *Oceanogr Mar Biol* 49:1–42.
8. Doney SC, Fabry VJ, Feely RA, Kleypas JA (2009) Ocean acidification: The other $CO_2$ problem. *Annu Rev Mar Sci* 1:169–192.
9. Dupont S, Ortega-Martínez O, Thorndyke M (2010) Impact of near-future ocean acidification on echinoderms. *Ecotoxicology* 19(3):449–462.
10. Kroeker KJ, et al. (2013) Impacts of ocean acidification on marine organisms: Quantifying sensitivities and interaction with warming. *Glob Change Biol* 19(6):1884–1896.
11. Stumpp M, Wren J, Melzner F, Thorndyke MC, Dupont ST (2011) $CO_2$ induced seawater acidification impacts sea urchin larval development I: Elevated metabolic rates decrease scope for growth and induce developmental delay. *Comp Biochem Physiol A Mol Integr Physiol* 160(3):331–340.
12. Stumpp M, et al. (2012) Acidified seawater impacts sea urchin larvae pH regulatory systems relevant for calcification. *Proc Natl Acad Sci USA* 109(44):18192–18197.
13. Stumpp M, et al. (2013) Digestion in sea urchin larvae impaired under ocean acidification. *Nat Clim Chang* 3(12):1044–1049.
14. Waldbusser GG, et al. (2015) Saturation-state sensitivity of marine bivalve larvae to ocean acidification. *Nat Clim Chang* 5(3):273–280.
15. Kurihara H, Shirayama Y (2004) Effects of increased atmospheric $CO_2$ on sea urchin early development. *Mar Ecol Prog Ser* 274:161–169.
16. Dorey N, Lançon P, Thorndyke M, Dupont S (2013) Assessing physiological tipping point of sea urchin larvae exposed to a broad range of pH. *Glob Change Biol* 19(11): 3355–3367.
17. Pespeni MH, et al. (2013) Evolutionary change during experimental ocean acidification. *Proc Natl Acad Sci USA* 110(17):6937–6942.
18. Pace DA, Manahan DT (2006) Fixed metabolic costs for highly variable rates of protein synthesis in sea urchin embryos and larvae. *J Exp Biol* 209(1):158–170.
19. Gnaiger E (1983) *Polarographic Oxygen Sensors: Aquatic and Physiological Applications*, eds Gnaiger E, Forstner H (Springer, New York), pp 337–345.
20. Shilling FM, Manahan DT (1990) Energetics of early development for the sea urchins *Strongylocentrotus purpuratus* and *Lytechinus pictus* and the crustacean *Artemia sp*. *Mar Biol* 106(1):119–127.
21. Sokolova IM, Frederich M, Bagwe R, Lannig G, Sukhotin AA (2012) Energy homeostasis as an integrative tool for assessing limits of environmental stress tolerance in aquatic invertebrates. *Mar Environ Res* 79:1–15.
22. Matson PG, Yu PC, Sewell MA, Hofmann GE (2012) Development under elevated $pCO_2$ conditions does not affect lipid utilization and protein content in early life-history stages of the purple sea urchin, *Strongylocentrotus purpuratus*. *Biol Bull* 223(3): 312–327.
23. Hochachka PW, Somero GN (2002) *Biochemical Adaptation: Mechanism and Process in Physiological Evolution* (Oxford Univ Press, New York, NY), 466 pp.
24. Cole BJ, Hamdoun A, Epel D (2013) Cost, effectiveness and environmental relevance of multidrug transporters in sea urchin embryos. *J Exp Biol* 216(20):3896–3905.
25. Rolfe DF, Brown GC (1997) Cellular energy utilization and molecular origin of standard metabolic rate in mammals. *Physiol Rev* 77(3):731–758.
26. Berg WE, Mertes DH (1970) Rates of synthesis and degradation of protein in the sea urchin embryo. *Exp Cell Res* 60(2):218–224.
27. Schubert U, et al. (2000) Rapid degradation of a large fraction of newly synthesized proteins by proteasomes. *Nature* 404(6779):770–774.
28. Pace DA, Maxson R, Manahan DT (2010) Ribosomal analysis of rapid rates of protein synthesis in the Antarctic sea urchin *Sterechinus neumayeri*. *Biol Bull* 218(1):48–60.
29. Sherman MY, Qian SB (2013) Less is more: Improving proteostasis by translation slow down. *Trends Biochem Sci* 38(12):585–591.
30. Escusa-Toret S, Vonk WIM, Frydman J (2013) Spatial sequestration of misfolded proteins by a dynamic chaperone pathway enhances cellular fitness during stress. *Nat Cell Biol* 15(10):1231–1243.
31. Pace DA, Manahan DT (2007) Efficiencies and costs of larval growth in different food environments (asteroidea: *Asterina miniata*). *J Exp Mar Biol Ecol* 353(1):89–106.
32. Pace DA, Manahan DT (2007) Cost of protein synthesis and energy allocation during development of antarctic sea urchin embryos and larvae. *Biol Bull* 212(2):115–129.
33. Marsh AG, Maxson RE, Jr, Manahan DT (2001) High macromolecular synthesis with low metabolic cost in Antarctic sea urchin embryos. *Science* 291(5510):1950–1952.
34. Hawkins AJS, Widdows J, Bayne BL (1989) The relevance of whole-body protein metabolism to measured costs of maintenance and growth in *Mytilus edulis*. *Physiol Zool* 62(3):745–763.
35. Fuery CJ, Withers PC, Guppy M (1998) Protein synthesis in the liver of *Bufo marinus*: Cost and contribution to oxygen consumption. *Comp Biochem Physiol A Mol Integr Physiol* 119(2):459–467.
36. Storch D, Pörtner HO (2003) The protein synthesis machinery operates at the same expense in eurythermal and cold stenothermal pectinids. *Physiol Biochem Zool* 76(1): 28–40.
37. Hwang PP (2009) Ion uptake and acid secretion in zebrafish (*Danio rerio*). *J Exp Biol* 212(11):1745–1752.
38. Melzner F, et al. (2009) Physiological basis for high $CO_2$ tolerance in marine ectothermic animals: Pre-adaptation through lifestyle and ontogeny? *Biogeosciences* 6(10):2313–2331.
39. Wright SH, Manahan DT (1989) Integumental nutrient uptake by aquatic organisms. *Annu Rev Physiol* 51(1):585–600.
40. Schwanhäusser B, et al. (2011) Global quantification of mammalian gene expression control. *Nature* 473(7347):337–342.
41. Marsh AG, Leong PKK, Manahan DT (2000) Gene expression and enzyme activities of the sodium pump during sea urchin development: Implications for indices of physiological state. *Biol Bull* 199(2):100–107.
42. Feder ME, Walser JC (2005) The biological limitations of transcriptomics in elucidating stress and stress responses. *J Evol Biol* 18(4):901–910.
43. Suarez RK, Moyes CD (2012) Metabolism in the age of 'omes'. *J Exp Biol* 215(14): 2351–2357.
44. Yang TH, Somero GN (1996) Activity of lactate dehydrogenase but not its concentration of messenger RNA increases with body size in barred sand bass, *Paralabrax nebulifer* (Teleostei). *Biol Bull* 191(2):155–158.
45. Hand SC (1999) *Handbook of Thermal Analysis and Calorimetry*, ed Kemp RB (Elsevier Science, Amsterdam), Vol 4, pp 469–510.
46. Leong PKK, Manahan DT (1997) Metabolic importance of $Na^+/K^+$-ATPase activity during sea urchin development. *J Exp Biol* 200(22):2881–2892.
47. Thomsen J, Casties I, Pansch C, Körtzinger A, Melzner F (2013) Food availability outweighs ocean acidification effects in juvenile *Mytilus edulis*: Laboratory and field experiments. *Glob Change Biol* 19(4):1017–1027.
48. Shilling FM, Manahan DT (1994) Energy metabolism and amino acid transport during early development of Antarctic and temperate echinoderms. *Biol Bull* 187(3):398–407.
49. Moran AL, Manahan DT (2004) Physiological recovery from prolonged 'starvation' in larvae of the Pacific oyster *Crassostrea gigas*. *J Exp Mar Biol Ecol* 306(1):17–36.

# Supporting Information

## Pan et al. 10.1073/pnas.1416967112

### SI Calculations and Estimations

**Allocation of Metabolic Energy to Protein Synthesis.** The proportion of metabolic energy allocated to protein synthesis was calculated using the measured energy cost per unit of protein synthesized (Fig. 3*C*, grand mean). For example, the rate of protein synthesis for 2-d-old embryos under control treatment was 0.4 ± 0.04 nanograms protein per individual per hour (Table S4, first row). Based upon the measured cost of protein synthesis of 2.4 J/mg protein synthesized, the metabolic cost of synthesizing protein at this rate is 0.86 microJoules per individual per hour. The corresponding metabolic rate for these 2-d-old embryos was 5.2 ± 0.33 picomoles $O_2$ per individual per hour, equivalent to 2.5 microJoules per individual per hour [484 J/mmol $O_2$ (1)]. Hence, protein synthesis accounted for 34% of the metabolic rate (Fig. 5*A*, control 2-d-old embryos). Similar sets of calculations from Table S4 form the basis of ATP allocation pie charts in Fig. 5.

**Allocation of Metabolic Energy to Ion Transport.** The proportion of metabolic energy allocated to in vivo ion transport activity of $Na^+$,$K^+$-ATPase was calculated by converting values of $K^+$ transport to ATP equivalents. The ATP equivalents of sodium–potassium transport activity by $Na^+$,$K^+$-ATPase have been established previously for developmental stages of *S. purpuratus* (2). Two moles of $K^+$ are transported by $Na^+$,$K^+$-ATPase for every mole of ATP hydrolyzed, allowing the conversion of the ion transport rate to ATP equivalents. Metabolic rates were converted to ATP equivalents using 5.2 pmol ATP/pmol $O_2$ (3).

**Fractional Rates of Protein Turnover.** For developmental stages in which no exogenous feeding on particulate foods occurs, and for which there is no net protein growth (e.g., embryos), measured rates of protein synthesized are equivalent to rates of protein turnover. Fractional rates of protein synthesis, i.e., (protein synthesis rate/whole-body protein content) × 100, represent the percentage of total body protein turned over per unit of time. One- and 2-d-old embryos had an average protein content of 18.5 ng per embryo and a protein synthesis rate of 0.4 ng per embryo per hour (Fig. 2). For these stages, the fractional rate of protein turnover is 2.2%/h.

**Accounting for the Increase in Metabolic Rate of Unfed Larvae.** The metabolic rates of unfed 6- to 10-d-old larvae increased from an average of 5.7 picomoles $O_2$ per larva per hour in controls to 7.8 picomoles $O_2$ per larva per hour under acidification treatment (Fig. 1*B*, *Inset*), an increase of 2.1 picomoles $O_2$ per larva per hour. To convert oxygen use to energy, an oxyenthalpic equivalent of 484 J/mmol $O_2$ was used, because developing sea urchins have lipid and protein as the dominant biochemical constituents (4). The increase in metabolic rate corresponds to an increase of 1.0 microJoules per larva per hour. In unfed larvae from the same cultures, rates of protein synthesis increased from 0.19 nanograms per larva per hour under control conditions to 0.37 nanograms per larva per hour under acidification treatment (Fig. 2*B*, *Inset*). Using the measured cost per unit of protein synthesis, the approximately twofold increase in the synthesis rate of unfed larvae is equivalent to 0.43 microJoules per larva per hour [(0.37–0.19) × 2.4 μJ/ng protein] (Fig. 3*C*). Hence, the increased rate of protein synthesis under acidification accounts for 43% of the increase in metabolic rate of 1.0 microJoules per larva per hour. In unfed larvae subjected to acidification treatment, in vivo $Na^+$,$K^+$-ATPase activity increased to 14.0 picomoles ATP per larva per hour from 7.0 ATP per larva per hour under control conditions. Converting this increase of 7.0 picomoles ATP per larva per hour to oxygen equivalents [5.2 pmol ATP/pmol $O_2$ (3)] results in an incremental value for the metabolic cost of ion transport of 1.3 picomoles $O_2$ per larva per hour. Hence, this increased rate under acidification accounts for 62% of the increase in metabolic rate (1.3 pmol $O_2$ = 62% of 2.1 pmol $O_2$). Combined, the energy demand of increased rates of protein synthesis (43%) and ion transport (62%) fully account for the observed increase in metabolic rate (i.e., 105%, within reasonable experimental error) in unfed larvae under acidification.

### SI Materials and Methods

**Animal Culturing and Biological and Technical Replications.** A total of 16 million eggs combined from four females were fertilized with pooled sperm from four males. Fertilized eggs were randomly assigned to stock four 200-L culture vessels at 20 eggs/mL. Two of these culture vessels contained control seawater (~400 μatm $pCO_2$) (Table S1), and two contained $CO_2$-pretreated seawater (~800 μatm $pCO_2$). Once the feeding stage was reached on day 4, aliquots of larvae were removed from the control and acidified seawater cultures and were resuspended in a series of eight 20-L cultures at an initial stocking density of 10 larvae/mL. The density was reduced to ~2 larvae/mL as development proceeded and samples were removed from culture vessels for analyses. Four of these 20-L culture vessels at ~400 μatm $pCO_2$ were treated further by the presence or absence of algal food (fed and unfed treatments). Similar feeding treatments were conducted on larvae at ~800 μatm $pCO_2$. For all feeding and $pCO_2$ treatments, measurements of body size, metabolic rate, protein synthesis rate, and in vivo $Na^+$,$K^+$-ATPase activity were made on embryos and prefeeding, fed and unfed larvae (ranging in age from 1- to 10-d-old individuals). Approximately 50,000 individuals were analyzed each day of sampling (see Table S4 for details of measurements). Additional batches of 1,000 to 5,000 individuals (depending upon developmental stage) were frozen at −80 °C for later analyses of total $Na^+$,$K^+$-ATPase, enzyme, and gene-expression assays. This entire protocol was repeated for 1- to 14-d-old individuals with the exception of the unfed treatment, using pooled gametes obtained from an additional set of three females and two males. Replicate cohorts of developing sea urchins were included in all statistical analyses; cohorts did not differ in body length or metabolic rate (Table S3).

For experiments measuring the cost of protein synthesis, a total of four cohorts of developmental stages obtained from different sets of parents were used. Concurrent measurements of metabolic rate and protein synthesis were made on 1-, 4-, 6-, and 10-d-old embryos and larvae, with and without emetine. To obtain the grand mean for the cost of protein synthesis given in Fig. 3*C*, nine cost values were determined based on nine sets of metabolic rates (with up to 10 replicate respiration measurements each) and nine sets of protein synthesis rates (with up to three five-point time-course assays each, e.g., Fig. 3*A*).

**Larval Size.** Growth rate was determined by measuring the diameter of 1- and 2-d-old embryos or midline body lengths of 3- to 14-d-old larvae. At least 50 randomly selected individuals from each treatment on each sampling day were measured in size-calibrated digital images from photomicroscopy. Digital images were analyzed using Image J software and converted to sizes in micrometers.

**Metabolic Rate.** Metabolic rates were determined from $O_2$ consumption using microrespiration measurements as previously described (5). Known numbers of individuals were incubated for 3–4 h in air-tight microrespiration vials containing filtered seawater that had been pre-equilibrated with either ambient air or elevated $pCO_2$. At the end of the incubation, the amount of $O_2$ was measured in samples taken from each respiration vial by injecting subsamples of 200 μL seawater into a temperature-controlled microcell (MC100; Strathkelvin) that was fitted with a polarographic oxygen sensor (Model 1302; Strathkelvin). Changes in the partial pressure of oxygen were monitored on an oxygen meter (Model 782; Strathkelvin) that was calibrated to the concentration of oxygen in moles/L.

**Protein Content.** Whole-body protein content was determined using the Bradford dye-binding assay, modified for developing marine invertebrates (6).

**Protein Synthesis Rate.** Absolute rates of protein synthesis were determined following the methods described previously for developing sea urchins (7). In each assay, known numbers of individuals were incubated in 10 mL of filtered seawater containing 74 kBq $^{14}$C-alanine (Perkin-Elmer Inc.) and adjusted to a final concentration of 10 μM alanine with cold carrier (nonradioactive alanine; Sigma-Aldrich). A series of 1-mL subsamples of individuals in the incubation seawater was collected approximately every 6 min and gently filtered through a filter membrane (pore size, 8 μm; Nucleopore). Animals were retained on the membrane, gently rinsed with 10 mL of seawater to removed excess radioactivity, and immediately frozen at −80 °C until further analysis. The amount of $^{14}$C-alanine incorporated into trichloroacetic acid (TCA)-precipitatable protein at each time interval was measured by scintillation counting and subsequently corrected, using HPLC analysis, for the intracellular specific activity of $^{14}$C-alanine in the free amino acids pool in each developmental stage. The amount of alanine incorporated into protein was converted to an absolute rate of protein synthesis. This calculation was based on the amino acid composition of the whole-body protein content of *S. purpuratus* (Table S2). The measured mole-percent–corrected molecular mass of amino acids in protein was 127.4 g/mole, and the mole-percent of alanine was 7.9%. Rates of protein synthesis were calculated from the slope of the linear regression describing the relationship between the amounts of newly synthesized protein and time.

**Cost of Protein Synthesis.** The cost of protein synthesis for developmental stages of *S. purpuratus* was determined by measuring the metabolic rate and protein synthesis rates in the absence and presence of the protein synthesis inhibitor (emetine at 100 μM). Emetine is a well-documented specific inhibitor of protein synthesis that does not affect other major ATP-consuming processes such as RNA synthesis in developing sea urchins (8) or whole-cell $Na^+$,$K^+$-ATPase activity in cell lines (9). The selected concentration of 100 μM has been shown to inhibit protein synthesis almost completely (Fig. 3*A*) (8) and has been used for several species of developing sea urchins (7, 10). This analysis of the cost of protein synthesis was extended further to measure the synthesis cost in *S. purpuratus* developing in different $pCO_2$ treatments.

**In Vivo $Na^+$,$K^+$-ATPase Activity.** The physiologically active fraction of total $Na^+$,$K^+$-ATPase in the developmental stages of *S. purpuratus* was measured as the ouabain-sensitive portion of potassium transport. The isotope $^{86}Rb^+$ was used for this analysis, as previously described for *S. purpuratus* (2). Briefly, for a given developmental stage, a known number of embryos or larvae was placed in 10 mL of filtered seawater to which was added 0.9 MBq of $^{86}Rb^+$ (PerkinElmer, Inc.). A 1-mL subsample of individuals was removed from the seawater solution every 1–2 min and filtered through a filter membrane (pore size, 8 μm; Nucleopore). Animals on the membrane were rinsed gently with 10 mL of seawater to remove excess isotope. The membrane filter holding the biological sample was placed in a 7-mL liquid scintillation counting vial to which 0.5 mL of tissue solubilizer (Solvable; PerkinElmer, Inc.) was added. After overnight solubilization, liquid scintillation mixture was added, and the radioactivity in each vial was determined. The rate of ion transport was calculated from the slope of the linear regression describing the relationship between $^{86}Rb^+$ transport and incubation time. To convert this value to a rate of $K^+$ transport (and, hence, in vivo $Na^+$,$K^+$-ATPase activity), the rate of $^{86}Rb^+$ transport was corrected for the specific activity of $K^+$ in seawater, using salinity of 33.5‰ (Table S1).

**Total $Na^+$,$K^+$-ATPase Enzyme Activity.** Total activity was determined using published methods for developmental stages of *S. purpuratus* (2). Frozen embryos and larvae were homogenized in a 10% sucrose buffer. Approximately 30 μg of protein was used for each $Na^+$,$K^+$-ATPase enzyme assay. Subsamples of homogenates were placed at a ratio of 1:3 in a reaction buffer (130 mM NaCl, 20 mM KCl, 10 mM $MgCl_2$, 50 mM imidazole, 5 mM ATP, pH 7.7) in the presence or absence of 2 mM ouabain. Reaction mixtures were incubated at 25 °C for 20 min, and the production of inorganic phosphate from ATP was measured at 700 nm in a spectrophotometer.

**$Na^+$,$K^+$-ATPase Gene Expression.** Steady-state levels of *$Na^+$,$K^+$-ATPase α* were determined in real-time quantitative PCRs (qPCRs), normalized to that of *EF1α*. Total RNA was extracted using TRIzol reagent (Life Technologies) according to the manufacturer's instructions, treated with RNase-free DNase, and purified with a RNA Clean and Concentrator kit (Zymo Research). Samples were eluted from purification columns in nuclease-free water; RNA concentration in the eluate was determined from absorption at 260 nm, measured with a NanoDrop spectrophotometer (Thermo Scientific). DNA-free RNA was reverse transcribed to cDNA using SuperScript III reverse transcriptase (Life Technologies) and random hexamers. Reverse-transcribed cDNA then was diluted 1:5 with nuclease-free water. Steady-state levels of *S. purpuratus $Na^+$,$K^+$-ATPase α* (NM_001123510) were determined in real-time qPCR assays as described (11), using the following primer sequences: forward, GGTGGTCAATTTGACAAGTCTTCA; reverse, TCAGATCGGTTGCAGAGACAA. Expression of *$Na^+$,$K^+$-ATPase α* was normalized to that of *EF1α* (NM_001123497), assayed using the primer sequences: forward, CAACGAAATCGTCAGGGAGGTC; reverse, AGATTGGGATGAAGGGCACAG. Relative expression is presented as copies of *$Na^+$,$K^+$-ATPase α* per copy of *EF1α*. Copy number values were determined from a standard curve created using plasmids containing clones of *$Na^+$,$K^+$-ATPase α* or *EF1α*. All qPCR samples were assayed in duplicate. SYBR Advantage qPCR Premix (Clontech) was mixed with cDNA template, forward and reverse primers (0.2 μM each), and nuclease-free water to a final volume of 25 μL. Samples were cycled on a MX3005P thermocycler (Agilent Technologies, Inc.) as follows: initial denaturation for 30 s at 95 °C followed by 40 cycles of 5 s at 95 °C and 30 s at 60 °C.

**In Vivo $^{35}$S-Met/Cys Labeling of Proteins.** Three samples of 1,500 12-d-old larvae were taken from a cohort subjected to either control or acidification treatment. These larvae were radiolabeled in 1.5-mL test tubes for 4 h at 15 °C by the addition of 100 μCi of a protein-labeling mix ($^{35}$S-Met/Cys; Perkin-Elmer, Inc.), with 500 nM methionine added as cold carrier (Sigma Chemical Co.) to seawater. At the end of the incubation, larvae were gently centrifuged, the seawater and unincorporated isotope were removed, and the pelleted larvae were washed with filtered seawater (three low-speed centrifugation washing cycles) to remove

excess radioactivity. Samples were stored at −80 °C until prepared for analysis by PAGE. Samples were homogenized in radioimmunoprecipitation assay (RIPA) buffer (150 mM NaCl, 0.1% Triton X-100, 0.5% sodium deoxycholate, 0.1% SDS, 50 mM Tris·HCl, pH 8.0). Protein was precipitated from tissue homogenates by the addition of cold TCA (5% final concentration), incubated for 1 h on ice, and centrifuged for 15 min at 14,000 × *g* (4 °C). Supernatant containing the unincorporated $^{35}$S-labeled amino acids was removed. The TCA-precipitated pellet was washed three times with 5% TCA to remove any excess radioactivity, followed by a final wash with methanol to remove residual TCA. Residual methanol was evaporated, and the protein pellet was resolubilized in 10 μL of 0.2 M NaOH. RIPA buffer was added to the resolubilized protein to a final volume of 100 μL. Radioactivity in protein samples was determined by liquid scintillation counting. Volumes containing equal amounts of radioactivity (counts: 75,000 dpm per electrophoretic lane) were combined with Laemmli loading dye (1:1), heated at 80 °C for 5 min, and immediately cooled on ice. Samples were loaded into an SDS polyacrylamide gel (4% stacking; 10% resolving) and separated by electrophoresis at 150 V for ∼2 h. The gel was stained with Coomassie Blue, incubated overnight in 5% glycerol, and then dried onto Whatman filter paper (70 °C for 4 h). The gel was exposed to a phosphoimager plate for 24 h; the plate was scanned with a Molecular Dynamics Storm 860 detection system (GE Healthcare).

**Statistical Analyses.** When a statistically significant relationship occurred between a biological response and size or age (e.g., regression of increase in metabolic rate with size in growing larvae), ANCOVA was used to test for differences between treatments. In other cases (e.g., absence of growth of unfed larvae), groups were compared by ANOVA. Where necessary, data were log transformed before ANCOVA (indicated in Table S3). Tukey tests were used for post hoc analyses.


1. Gnaiger E (1983) *Polarographic Oxygen Sensors: Aquatic and Physiological Applications*, eds Gnaiger E, Forstner H (Springer, New York), pp 337–345.
2. Leong PKK, Manahan DT (1997) Metabolic importance of $Na^+/K^+$-ATPase activity during sea urchin development. *J Exp Biol* 200(22):2881–2892.
3. McGilvery RW (1979) *Biochemistry: A functional approach* (W B Saunders, Philadelphia), 769 pp.
4. Shilling FM, Manahan DT (1994) Energy metabolism and amino acid transport during early development of Antarctic and temperate echinoderms. *Biol Bull* 187(3):398–407.
5. Marsh AL, Manahan DT (1999) A method for accurate measurements of the respiration rates of marine invertebrate embryos and larvae. *Mar Ecol Prog Ser* 184:1–10.
6. Jaeckle WB, Manahan DT (1989) Growth and energy imbalance during the development of a lecithotrophic molluscan larva (*Haliotis rufescens*). *Biol Bull* 177(2): 237–246.
7. Pace DA, Manahan DT (2006) Fixed metabolic costs for highly variable rates of protein synthesis in sea urchin embryos and larvae. *J Exp Biol* 209(1):158–170.
8. Hogan B, Gross PR (1971) The effect of protein synthesis inhibition on the entry of messenger RNA into the cytoplasm of sea urchin embryos. *J Cell Biol* 49(3):692–701.
9. Kennedy BG, Lever JE (1985) Transport by the ($Na^+$,$K^+$) ATPase: Modulation by differentiation inducers and inhibition of protein synthesis in the MDCK kidney epithelial cell line. *J Cell Physiol* 123(3):410–416.
10. Pace DA, Manahan DT (2007) Cost of protein synthesis and energy allocation during development of antarctic sea urchin embryos and larvae. *Biol Bull* 212(2):115–129.
11. Stumpp M, Dupont S, Thorndyke MC, Melzner F (2011) $CO_2$ induced seawater acidification impacts sea urchin larval development II: Gene expression patterns in pluteus larvae. *Comp Biochem Physiol A Mol Integr Physiol* 160(3):320–330.


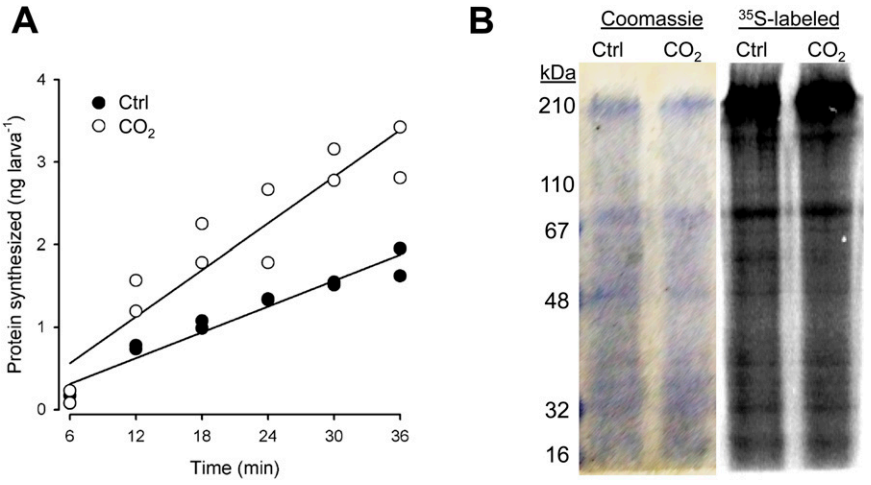


**Fig. S1.** Rates and patterns of protein synthesis in 12-d-old fed sea urchin larvae under control (Ctrl) and seawater acidification ($CO_2$) conditions. (*A*) Acidification resulted in an increased rate of protein synthesis compared with control (comparison of slopes, $P = 0.003$). (*B*) Representative images of PAGE separation of total proteins (Coomassie Blue stained) and autoradiogram of $^{35}$S-Met/Cys–labeled proteins. Equal amounts of radioactivity (in disintegrations/min) were loaded in each lane.

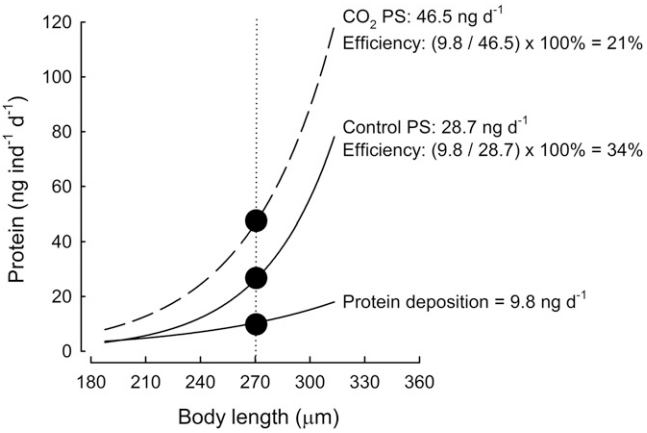


**Fig. S2.** Protein depositional efficiencies under control and seawater acidification treatments. Protein depositional efficiency (i.e., the ratio of protein accreted to protein synthesized) was calculated for a 270-μm larva, shown as a vertical dashed line near the midpoint of the regressions (calculated values are shown as solid circles). For developing sea urchins of this size, protein depositional efficiency was reduced to 21% under acidification, relative to 34% for those grown under control conditions. Calculations were based on equations for rates of protein deposition (9.8 ng/d) and protein synthesis (PS) under control (Control PS: 28.7 ng/d) and seawater acidification ($CO_2$ PS: 46.5 ng/d) conditions. Primary data are given in Fig. 2 *A* and *B*. The relationship between age and protein content of developing sea urchins in the current study is described by the regression equation: Protein content = $10.8 \times e^{(0.2 \times Age)}$ ($r^2 = 0.93$). The first derivative of this equation gives the equation for the daily rate of protein growth: rate of protein deposition = $10.8 \times 0.2 \times e^{(0.2 \times Age)}$. Body length was substituted for age using the equation for the regression shown in Fig. 1*A* (body length = $117.5 \times Age^{0.4}$). Daily rates of protein synthesis were calculated from the regression fit to the data in Fig. 2*B* [shown here on linear scale; Control: Log PS = 0.01 × (body length) − 1.4; Acidification: Log PS = 0.01 × (body length) − 0.8].

**Table S1. Environmental conditions in experimental cultures**

| Seawater parameter | Control | $CO_2$ treatment |
|---|---|---|
| Temperature, °C | 15.3 ± 0.10 | 15.3 ± 0.07 |
| $pH_{NBS}$ | 8.1 ± 0.01 | 7.9 ± 0.00 |
| Salinity | 33.5 | 33.5 |
| DIC, μmol/kg | 1,921.8 ± 53.33 | 2,180.1 ± 17.71 |
| $pCO_2$, μatm | 431.9 ± 16.78 | 800.6 ± 9.07 |
| Ω calcite | 3.1 ± 0.09 | 2.2 ± 0.02 |
| Ω aragonite | 2.0 ± 0.06 | 1.4 ± 0.02 |
| TA, μmol/kg | 2,097.1 ± 56.84 | 2,283.3 ± 18.18 |
| $CO_3^{2-}$, μmol/kg | 126.8 ± 4.93 | 90.7 ± 0.99 |

Temperature, pH (calibrated with National Bureau of Standards buffers, $pH_{NBS}$), and total dissolved inorganic carbon (DIC) are measured values. Temperature was monitored continuously throughout the duration of culture experiments with automatic temperature loggers that were placed in culture vessels (Model HOBO U12; Onset Computer Corp.). Measurements of pH and water samples for DIC were collected on each day of biological experiments. A handheld pH meter (Orion Star Handheld pH meter; Thermo Scientific), calibrated with National Institute of Standards and Technology standard was used for pH measurements. DIC was measured using a carbon coulometer (CM 5015; UIC, Inc.) calibrated with certified reference materials (batch 120) supplied by Andrew Dickson (Scripps Institution of Oceanography, San Diego). Salinity is from reported values for seawater near Santa Catalina Island where the seawater used for cultures was obtained (1). Total alkalinity (TA), partial pressure of $CO_2$ ($pCO_2$), calcite and aragonite saturation states, and carbonate ion ($CO_3^{2-}$) concentrations were calculated from measured variables using CO2SYS (2) with selected dissociation (3, 4) and $HSO_4^-$ constants (5). The average $pCO_2$ value (431.9 μatm) used to culture larvae under control conditions is within the range of values reported for coastal California waters (6). Values in the table are mean ± SEM. Ten culture vessels were assayed for carbonate chemistry throughout the developmental period studied, five for control and five for $CO_2$-treated seawater. The errors were calculated for $pCO_2$ for all statistical variation across culture vessels and between water sampling days and represent a maximum of 3.9% (SEM/mean) for control (431.9 μatm) and 1.1% for $CO_2$-treated (800.6 μatm) seawater. As expected, $pCO_2$ and pH differed significantly between treatments (Mann–Whitney *u* tests, $pCO_2$: $U = 0.0$, $P < 0.001$; pH: $U = 0.0$, $P < 0.001$). The values for TA calculated from CO2SYS are different by 8% ($U = 52.0$, $P < 0.001$) between treatments. By CO2SYS analysis, this 8% difference in TA for a given $pCO_2$ would change the reported pH values by no more than 0.036 units, thus not altering the major conclusion of this table showing a large difference in pH and $pCO_2$ between treatments.


1. Todd RE, Rudnick DL, Davis RE (2009) Monitoring the greater San Pedro Bay region using autonomous underwater gliders during fall of 2006. *J Geophys Res* 114:C06001.
2. Lewis E, Wallace D, Allison LJ (1998) *Program Developed for $CO_2$ System Calculations* (Oak Ridge National Laboratory, Oak Ridge, TN).
3. Mehrbach C, Culberson CH, Hawlwy JE, Pytkowicz RM (1973) Measurement of the apparent dissociation constants of carbonic acid in seawater at atmospheric pressure. *Limnol Oceanogr* 18(6):897–907.
4. Dickson AG, Millero FJ (1987) A comparison of the equilibrium-constants for the dissociation of carbonic-acid in seawater media. *Deep-Sea Res* 34(10):1733–1743.
5. Dickson AG (1990) Standard potential of the reaction: AgCl(s) + 1/2$H_2$(g) = Ag(s) + HCl(aq), and the standard acidity constant of the ion $HSO_4^-$ in synthetic sea water from 273.15 to 318.15 K. *J Chem Thermodyn* 22(2):113–127.
6. Frieder CA, Nam SH, Martz TR, Levin LA (2012) High temporal and spatial variability of dissolved oxygen and pH in a nearshore California kelp forest. *Biogeosciences* 9(10):3917–3930.

**Table S2. Amino acid composition of proteins in developmental stages of the sea urchin *S. purpuratus* under control and seawater acidification treatments**

| Protein | Control treatment, nmoles | | | | Acidification treatment, nmoles | | | Grand mean, nanomoles | Composition of protein, mole-percent |
|---|---|---|---|---|---|---|---|---|---|
| | Day 1 | Day 4 | Day 9 | Day 14 | Day 1 | Day 4 | Day 14 | | |
| Tryptophan | 0.9 | 0.7 | | | | 0.8 | | 0.8 ± 0.07 | 0.8 |
| Cysteine | 1.0 | 0.9 | | 1.1 | 1.1 | 1.0 | | 1.0 ± 0.04 | 1.0 |
| Methionine | 1.4 | 1.2 | | 1.5 | 1.4 | 1.3 | 1.6 | 1.4 ± 0.06 | 1.4 |
| Histidine | 1.7 ± 0.01 | 1.6 ± 0.01 | 1.9 ± 0.05 | 1.9 ± 0.03 | 1.7 ± 0.02 | 1.6 ± 0.04 | 1.9 ± 0.02 | 1.8 ± 0.03 | 1.7 |
| Tyrosine | 3.0 ± 0.04 | 3.0 ± 0.04 | 3.1 ± 0.04 | 3.2 ± 0.06 | 3.0 ± 0.01 | 3.1 ± 0.05 | 3.2 ± 0.02 | 3.1 ± 0.02 | 3.0 |
| Phenylalanine | 4.3 ± 0.06 | 4.3 ± 0.06 | 4.1 ± 0.05 | 4.2 ± 0.07 | 4.4 ± 0.02 | 4.4 ± 0.05 | 4.3 ± 0.03 | 4.3 ± 0.03 | 4.2 |
| Arginine | 4.7 ± 0.03 | 4.3 ± 0.01 | 5.2 ± 0.05 | 5.0 ± 0.08 | 4.8 ± 0.01 | 4.6 ± 0.12 | 5.1 ± 0.07 | 4.8 ± 0.07 | 4.7 |
| Proline | 5.0 ± 0.02 | 5.7 ± 0.11 | 5.1 ± 0.03 | 5.1 ± 0.09 | 5.0 ± 0.00 | 5.4 ± 0.04 | 5.0 ± 0.04 | 5.2 ± 0.06 | 5.1 |
| Isoleucine | 5.3 ± 0.07 | 5.1 ± 0.05 | 4.9 ± 0.04 | 5.1 ± 0.07 | 5.4 ± 0.04 | 5.2 ± 0.05 | 5.1 ± 0.02 | 5.2 ± 0.04 | 5.1 |
| Threonine | 6.5 ± 0.06 | 7.1 ± 0.10 | 5.9 ± 0.03 | 6.0 ± 0.05 | 6.6 ± 0.01 | 7.0 ± 0.03 | 5.9 ± 0.03 | 6.4 ± 0.11 | 6.3 |
| Serine | 6.8 ± 0.04 | 6.9 ± 0.04 | 6.5 ± 0.05 | 6.2 ± 0.06 | 6.9 ± 0.01 | 6.7 ± 0.07 | 6.3 ± 0.09 | 6.6 ± 0.06 | 6.5 |
| Lysine | 7.0 ± 0.07 | 5.9 ± 0.03 | 7.3 ± 0.12 | 7.0 ± 0.11 | 6.7 ± 0.42 | 6.0 ± 0.08 | 7.2 ± 0.07 | 6.7 ± 0.13 | 6.6 |
| Valine | 7.4 ± 0.10 | 7.1 ± 0.09 | 6.5 ± 0.01 | 6.6 ± 0.09 | 7.3 ± 0.05 | 7.1 ± 0.02 | 6.6 ± 0.02 | 6.9 ± 0.08 | 6.8 |
| Leucine | 8.3 ± 0.11 | 7.3 ± 0.07 | 7.6 ± 0.07 | 7.9 ± 0.13 | 8.5 ± 0.03 | 7.5 ± 0.11 | 8.1 ± 0.08 | 7.9 ± 0.09 | 7.8 |
| Alanine | 7.6 ± 0.06 | 8.2 ± 0.04 | 8.3 ± 0.04 | 8.1 ± 0.05 | 7.6 ± 0.04 | 8.1 ± 0.04 | 8.2 ± 0.04 | 8.0 ± 0.06 | 7.9 |
| Glycine | 8.0 ± 0.05 | 9.7 ± 0.06 | 11.0 ± 0.03 | 10.2 ± 0.13 | 7.9 ± 0.04 | 9.5 ± 0.06 | 10.1 ± 0.13 | 9.5 ± 0.24 | 9.4 |
| Aspartate/asparagine[†] | 10.7 ± 0.09 | 10.3 ± 0.12 | 10.8 ± 0.18 | 10.7 ± 0.05 | 10.5 ± 0.12 | 10.4 ± 0.02 | 10.1 ± 0.68 | 10.5 ± 0.10 | 10.4 |
| Glutamate/glutamine[†] | 11.8 ± 0.09 | 11.9 ± 0.06 | 10.9 ± 0.09 | 10.9 ± 0.07 | 11.8 ± 0.05 | 11.6 ± 0.01 | 10.9 ± 0.04 | 11.4 ± 0.10 | 11.2 |
| $MW_p$, g/mole | | | | | | | | | 127.4 |

The total number of protein samples analyzed for amino acid composition was 21 for the range of developmental stages, ages, and $pCO_2$ treatments given above (see Table S1 for chemistry conditions of control and seawater acidification treatments). The average molecular weight of amino acids in proteins ($MW_p$) of *S. purpuratus* was calculated to be 127.4 g/mole. This value was calculated from the grand mean of the 20 protein amino acids analyzed. The grand mean column represents average moles of amino acid present in developmental stages. Within replicate samples, the mass of protein sample that was acid-hydrolyzed before each amino acid analysis differed slightly. After analysis, the resultant moles of amino acids were normalized across different samples to a total of 100 nmol per sample. The $^{14}C$-labeled tracer used for determination of absolute rates of protein synthesis was alanine, which is present at 7.9 mole-percent in protein. Seawater acidification had no significant effect on amino acid composition of proteins in developmental stages, compared with control samples ($P > 0.05$). Data in each column labeled by Day are mean values ± 1 SEM, $n = 3$. For the column labeled Grand mean, values are mean ± 1 SEM for the pooled samples of all days and treatments ($n = 21$ for all amino acids other than tryptophan, $n = 3$; cysteine, $n = 5$; methionine, $n = 6$). Separate preparatory steps for amino acid analyses were conducted for individual measurements of tryptophan (mercaptoethanesulfonic acid hydrolysis), and cysteine and methionine (performic acid oxidation) as per standard protocols for amino acid analysis conducted at the University of California, Davis, Proteomics Core Facility where this analysis was conducted.

[†]Asparagine and glutamine form aspartate and glutamate, respectively, during the acid hydrolysis analysis step.

**Table S3. ANCOVA and ANOVA results for measured variables in developmental stages of the sea urchin *S. purpuratus* under control and seawater acidification treatments**

| | Source | df | F | *P* |
|---|---|---|---|---|
| ANCOVA variable | | | | |
| Body length*, Fig. 1*A* | Model | 3, 2,080 | 7,009.30 | <0.001 |
| | Age | 1 | 13,940.10 | <0.001 |
| | pH | 1 | 2.78 | 0.095 |
| | Cohort | 1 | 2.91 | 0.088 |
| Metabolic rate*, Fig. 1*B* | Model | 3, 254 | 731.70 | <0.001 |
| | Body length | 1 | 1,205.79 | <0.001 |
| | pH | 1 | 0.97 | 0.326 |
| | Cohort | 1 | 1.75 | 0.187 |
| Total protein content*, Fig. 2*A* | Model | 2, 48 | 189.10 | <0.001 |
| | Body length | 1 | 378.17 | <0.001 |
| | pH | 1 | 0.04 | 0.847 |
| Protein synthesis rate*, Fig. 2*B* | Model | 2, 19 | 56.79 | <0.001 |
| | Body length | 1 | 104.85 | <0.001 |
| | pH | 1 | 8.73 | 0.009 |
| Ion transport rate, Fig. 4*B* | Model | 2, 19 | 34.07 | <0.001 |
| | Body length | 1 | 61.02 | <0.001 |
| | pH | 1 | 7.12 | 0.016 |
| ANOVA variable | | | | |
| Body length, Fig. 1*A* | Model | 7, 480 | 11.35 | <0.001 |
| | Age | 3 | 25.65 | <0.001 |
| | pH | 1 | 0.38 | 0.537 |
| | Age × pH | 3 | 0.71 | 0.544 |
| Metabolic rate, Fig. 1*B* and *Inset* | Model | 3, 96 | 17.25 | <0.001 |
| | Stage† | 1 | 26.53 | <0.001 |
| | pH | 1 | 18.81 | <0.001 |
| | Stage × pH | 1 | 2.06 | 0.155 |
| Total protein content, Fig. 2*A* and *Inset* | Model | 3, 48 | 5.14 | <0.001 |
| | Stage† | 1 | 0.11 | 0.743 |
| | pH | 1 | 3.60 | 0.063 |
| | Stage × pH | 1 | 9.00 | 0.004 |
| Protein synthesis rate, Fig. 2*B* and *Inset* | Model | 3, 19 | 14.11 | <0.001 |
| | Stage† | 1 | 21.48 | 0.003 |
| | pH | 1 | 8.07 | 0.012 |
| | Stage × pH | 1 | 8.62 | 0.010 |
| Ion transport rate, Fig. 4*B* and *Inset* | Model | 3, 15 | 11.27 | 0.008 |
| | Stage† | 1 | 15.78 | 0.002 |
| | pH | 1 | 8.20 | 0.014 |
| | Stage x pH | 1 | 9.83 | 0.009 |
| $Na^+$,$K^+$-ATPase gene expression, Fig. 4*C* | Model | 11, 47 | 5.35 | <0.001 |
| | Age | 5 | 6.74 | 0.002 |
| | pH | 1 | 4.16 | 0.049 |
| | Age × pH | 5 | 4.25 | 0.004 |
| Total $Na^+$,$K^+$-ATPase activity, Fig. 4*C* | Model | 11, 37 | 0.28 | 0.984 |
| | Age | 5 | 0.37 | 0.863 |
| | pH | 1 | 0.02 | 0.877 |
| | Age × pH | 5 | 0.25 | 0.936 |

As stated in *Materials and Methods*, ANCOVA was used to test for differences between treatments when a statistically significant relationship occurred between a biological response and size or age (e.g., Fig. 1*B*, regression of increase in metabolic rate with size in growing larvae). In other cases (e.g., Fig. 1*A*, absence of growth of unfed larvae), groups were compared by ANOVA. If significant interactions are evident, post hoc Tukey analyses were performed. The term "cohort" refers to groups of developmental stages obtained from different parents and used in replicate sets of experimental treatments and measurements.

*Log-transformed data.

†Stage includes embryos and unfed larvae.

**Table S4. The allocation of ATP to protein synthesis and ion regulation in developmental stages of the sea urchin *S. purpuratus* under control and seawater acidification treatments and under different feeding states**

| $CO_2$ treatment | Feeding state | Age, d | Body length, μm | Metabolic rate, picomoles $O_2$ per individual per hour | Protein synthesis rate, nanograms protein per individual per hour | ATP allocation to protein synthesis, % | In vivo $Na^+,K^+$-ATPase activity, picomoles $P_i$ per individual per hour | ATP allocation to $Na^+,K^+$-ATPase, % | Unaccounted fraction, % |
|---|---|---|---|---|---|---|---|---|---|
| Control | Prefeeding | 2 | 145.6 ± 1.93 | 5.2 ± 0.33 | 0.4 ± 0.04 | 34 | 4.1 | 15 | 51 |
| | | 3 | 194.0 ± 2.36 | 7.7 ± 0.71 | 0.3 ± 0.03 | 18 | 4.6 | 12 | 70 |
| | | 4 | 222.3 ± 1.62 | 6.7 ± 0.40 | 0.3 ± 0.02 | 19 | 5.3 | 15 | 66 |
| | Fed | 6 | 253.6 ± 1.87 | 14.1 ± 1.14 | 0.9 ± 0.08 | 31 | 18.6 | 25 | 44 |
| | | 8 | 282.1 ± 2.71 | 23.2 ± 1.28 | 1.1 ± 0.39 | 24 | 27.4 | 23 | 53 |
| | | 10 | 318.5 ± 2.47 | 51.0 ± 2.59 | 5.3 ± 0.52 | 51 | 28.0 | 11 | 38 |
| | Unfed | 6 | 253.1 ± 2.01 | 5.0 ± 0.2 | 0.2 ± 0.03 | 21 | 7.8 | 30 | 49 |
| | | 8 | 260.0 ± 3.01 | 6.1 ± 0.3 | 0.2 ± 0.03 | 17 | 6.2 | 20 | 63 |
| Acidification | Prefeeding | 2 | 137.3 ± 1.46 | 7.2 ± 0.72 | 0.4 ± 0.06 | 25 | 8.0 | 22 | 53 |
| | | 3 | 203.8 ± 2.74 | 10.8 ± 1.40 | 0.7 ± 0.06 | 30 | 13.9 | 25 | 45 |
| | | 4 | 218.8 ± 1.50 | 7.3 ± 0.85 | 0.6 ± 0.16 | 41 | 10.6 | 28 | 31 |
| | Fed | 6 | 259.1 ± 1.90 | 11.5 ± 0.74 | 1.1 ± 0.14 | 46 | 21.1 | 35 | 19 |
| | | 8 | 288.1 ± 3.66 | 20.1 ± 1.12 | 2.4 ± 0.44 | 59 | 27.2 | 26 | 15 |
| | | 10 | 300.8 ± 3.66 | 42.6 ± 2.30 | 5.6 ± 0.50 | 66 | 45.3 | 20 | 14 |
| | Unfed | 6 | 252.7 ± 2.55 | 7.7 ± 0.16 | 0.4 ± 0.04 | 24 | 18.4 | 46 | 30 |
| | | 8 | 255.2 ± 2.69 | 6.0 ± 0.26 | 0.3 ± 0.03 | 26 | 14.1 | 45 | 29 |

Physiological rates used for the calculation of ATP allocation pie charts shown in Fig. 5. At each age, measurements were made on different aliquots of larvae from the same cohort of individuals cultured under control or acidification conditions. Data are shown as mean ± 1 SEM; $n = 50$ individuals for body midline length measurement; $n = 8$–10 respiration vials (up to 800 individuals in each vial) for metabolic rate. Each protein synthesis rate is the slope (± SE) of duplicate six-point time-course assays. A total of 192 time points (with known number of individuals at each point, ~1,000) were sampled for synthesis rates presented in this table. At each time point, the amount of newly synthesized protein is corrected for intracellular specific activity of $^{14}$C-alanine with HPLC. Each in vivo $Na^+,K^+$-ATPase activity is calculated as the difference between duplicate six-point time-course $^{86}Rb^+$ transport assays with ouabain and two assays without ouabain. A total of 384 time-point samples (with known number of individuals at each point, ~1,000) were collected for the calculation of physiological rates of ion transport by $Na^+,K^+$-ATPase. Because of the subtractive nature of the determination of in vivo $Na^+,K^+$-ATPase activity (difference in rates with and without ouabain), error analyses are not listed for the column in the table; however, each of these $^{86}Rb^+$ transport assays had an error of 20% or less (i.e., on average regression $r^2$ values = 0.80 for 64 time-course assays; see Fig. 4*A* for an example). Calculations of ATP allocation for rates of protein synthesis and ion transport are described in in *SI Calculations and Estimations*.